J. Physiol. (1983), **336**, *pp.* 511–526
With 10 text-figures
Printed in Great Britain

ACETYLCHOLINE-INDUCED CURRENT FLUCTUATIONS AND FAST EXCITATORY POST-SYNAPTIC CURRENTS IN RABBIT SYMPATHETIC NEURONES

BY V. A. DERKACH, A. A. SELYANKO AND V. I. SKOK
From the Bogomoletz Institute of Physiology, Kiev-24, 252024, U.S.S.R.

(*Received 26 January 1982*)

SUMMARY

1. Post-synaptic currents and responses to ionophoretically applied acetylcholine (ACh) were recorded at 34–37 °C from rabbit superior cervical ganglion neurones clamped at −80 mV membrane potential. Atropine (1 μM) was used to block muscarinic receptors.

2. The fast excitatory post-synaptic current (e.p.s.c.) reversed at $-9{\cdot}6 \pm 1{\cdot}7$ mV and decayed with a single exponential time course. The e.p.s.c. decay time constant, τ_d, was $4{\cdot}5 \pm 0{\cdot}3$ msec and increased as the membrane was hyperpolarized (e-fold increase in τ_d corresponded to 140 mV hyperpolarization). Miniature e.p.s.c.s (m.e.p.s.c.s) decayed with time constants similar to those of the e.p.s.c.

3. The decay of the e.p.s.c. was slowed by lowering temperature but remained a single exponential; the changes of τ_d with temperature followed the Arrhenius equation ($Q_{10} = 3{\cdot}7$).

4. In most of the neurones studied the analysis of ACh noise spectra revealed two kinetic components with mean time constants $\tau_{N_1} = 1{\cdot}1 \pm 0{\cdot}1$ msec and $\tau_{N_2} = 5{\cdot}0 \pm 0{\cdot}5$ msec. In a few neurones only the τ_{N_1} component was found. Similar two-component ACh noise spectra were observed in the neurones not treated with atropine. τ_{N_1} and τ_{N_2} components revealed temperature dependences similar to each other and close to that of τ_d.

5. The values of τ_{N_1} and τ_{N_2} and the ratio between the contributions of the τ_{N_1} and τ_{N_2} components to the ACh noise spectrum did not depend on the dose of ACh.

6. The single channel conductance is 36 ± 3 pS. A single ACh quantum opens about 150 ionic channels and the e.p.s.c. consists of 4–243 quanta.

7. It is suggested that in mammalian sympathetic ganglion neurones there are two types of nicotinic ACh receptor channels, with short and long lifetimes, and that the kinetics of e.p.s.c. and m.e.p.s.c. are determined by the activity of the longer lifetime channel type.

INTRODUCTION

The fast excitatory post-synaptic current (e.p.s.c.) in sympathetic ganglion neurones shows a single exponential decay with a time constant, τ_d, of about 4–5 msec (Kuba & Nishi, 1979; Selyanko, Derkach & Skok, 1979; MacDermott, Connor, Dionne

& Parsons, 1980). This time constant is much longer than that of the end-plate current decay (*cf.* Takeuchi & Takeuchi, 1959; Kordaš, 1972; Katz & Miledi, 1972; Magleby & Stevens, 1972*a*, *b*). The time constant of the end-plate current decay is equal to the mean lifetime of the ionic channels opened by synaptic transmitter (Katz & Miledi, 1972; Anderson & Stevens, 1973). If this is true for the sympathetic neurones, then the ionic channels must stay open for a much longer time than at the end-plate.

To test this, the channel lifetime in rabbit sympathetic neurones was estimated by analysing the membrane current fluctuations produced by exogenous acetylcholine (ACh noise). The results obtained suggest that there are two types of nicotinic ACh receptor channels in sympathetic ganglion neurones, one type with a mean lifetime corresponding to τ_d of the e.p.s.c. and miniature e.p.s.c. (m.e.p.s.c.), and another type with a markedly shorter mean single channel lifetime. In contrast to the ACh receptor channels recently studied in parasympathetic ganglion neurones (Rang, 1981), the channels with the shorter lifetime are probably *not* involved in synaptic transmission. Some of the present results have previously been reported (Derkach, Selyanko & Skok, 1981; Skok, Selyanko & Derkach, 1981).

METHODS

The experiments were performed on superior cervical ganglia rapidly isolated from rabbits killed by an air embolism during light ether anaesthesia. The ganglion was denuded of connective tissue and pinned out upon Sylgard transparent plastic in the bottom of the chamber. The chamber was perfused with a solution warmed to 34–37 °C and equilibrated with O_2 (95%) and CO_2 (5%). This solution had the following composition (mM): NaCl, 137·9; KCl, 4·0; $CaCl_2$, 2·0; $MgCl_2$, 0·5; KH_2PO_4, 1·0; $NaHCO_3$, 12·0; glucose, 11·0 (pH 7·4).

The impalement of a cell with two micropipettes for voltage clamping and the placement of the micro-ionophoretic pipette were observed under Nomarski differential interference optics at a total magnification of 400 × using a 40 × water immersion objective with a 1·6 mm working distance. Large cells (50–70 μm in diameter) were selected for impalement. For orthodromic stimulation, single current pulses were applied to the cervical sympathetic nerve close to the ganglion through a suction electrode. ACh was applied ionophoretically through a micropipette filled with acetylcholine chloride (2·5 M), with a resistance of no more that 50 MΩ and using current pulses not exceeding 20 nA in amplitude and 6–9 s in duration. Leakage was prevented with backing currents of about 5 nA. Both stimulating and ionophoretic currents were supplied through electro-optical isolation units. The tip of the ionophoretic micropipette was placed outside the connective tissue capsule of the cell, approximately 20 μm away from the surface of the cell, to minimize the possibility of local ACh concentration fluctuations near the cell surface that may influence the ACh noise spectrum. To avoid saturation and desensitization of ACh receptors, only weak ionophoretic currents producing membrane current fluctuations with variance linearly related to the amplitude of steady ACh-induced current were used.

Atropine (1 μM) was added to the perfusion solution to block muscarinic receptors, unless otherwise stated; no acetylcholinesterase inhibitors were used.

The cell was voltage clamped with two intracellular micropipettes filled with 3 M-KCl, with resistances of 20–50 MΩ. The voltage-clamp technique used was essentially the same as that described by Selyanko *et al.* (1979). The residual voltage change during e.p.s.c. usually was less than 5% of the driving potential. The current pulse following a testing command hyperpolarizing step of 10 mV decayed within 0·3–1·0 msec. E.p.s.c.s and m.e.p.s.c.s were recorded within the frequency ranges 0 to 900–1500 Hz and from 1 to 430 Hz, respectively. The spontaneously appearing m.e.p.s.c.s were recorded on the tape recorder and then captured by triggering the sweep with their rising phases. The results were obtained at a membrane potential of −80 mV unless otherwise indicated.

For noise analysis, the membrane current was recorded on a tape recorder with a low gain d.c. amplifier and a high gain a.c. amplifier within the frequency range 1–430 Hz. Four records, each

1 sec long, were taken before and four records during the ionophoretic application of ACh. For each record digitalized at 1 kHz sampling rate a power spectrum was obtained within the frequency range from 4 to 512 Hz using fast Fourier transform by SM-3 computer. The net ACh noise spectrum was obtained by subtracting an averaged control spectrum from an averaged ACh noise spectrum. Then the net ACh noise spectrum was smoothed by averaging in groups of six points. In most of the neurones studied control spectra were U-shaped with minimum at 100–150 Hz; in the remaining few neurones the spectral density decayed smoothly and did not increase within the frequency band used (up to 430 Hz). The net spectrum was fitted by one or, if necessary, two Lorentzian curves using a non-linear least squares fit computer program, within the frequency range from 4 to 350 Hz.

Because of the relatively high resistance of the voltage recording electrode, R_e, the main source of clamping current background noise is apparently the R_e thermal noise. Assuming the neurone soma is a sphere and modelling the membrane as a parallel RC network, the spectral density of this noise, $S(f)$ as a function of frequency, f, and its variance, σ^2, can be represented by

$$S(f) = 4\,kTR_e\left(\frac{1}{R_{in}^2} + 4\pi^2 f^2 C_{in}^2\right)$$

and

$$\sigma^2 = \int_{f_1}^{f_2} S(f)\,df,$$

where R_{in} and C_{in} are the input resistance and input capacitance of the cell; k, the Boltzmann constant; T, the temperature and f_1 and f_2 are the lower and upper limits of the frequency range analysed. With $T = 310$ K, $R_e = 40$ MΩ, $R_{in} = 10$ MΩ (mean value of R_{in} measured in four neurones was equal to 11·8 MΩ), C_{in} assumed to be equal to 10^{-9} F (Skok, 1973), $f_1 = 1$ Hz and $f_2 = 430$ Hz, σ^2 should be equal to 7×10^{-22} A², which was close to σ^2 of background noise observed in our experiment ($0{\cdot}9–2 \times 10^{-21}$ A²). This value of σ^2 for background noise usually was much lower than σ^2 for membrane current noise observed during the ACh effect ($7–30 \times 10^{-21}$ A²). However, the subtraction procedure described above was always used, which was especially needed in depolarized cells and at low doses of ACh. An additional noise component, produced by the ACh-induced decrease in R_{in} (which was in our experiments equal to approximately 50 % of resting R_{in}) could not be removed by the subtraction procedure. Its spectral density, Δ_S, and variance, $\Delta\sigma^2$, are

$$\Delta S = 4\,kTR_e\left(\frac{1}{R_{in}'^2} - \frac{1}{R_{in}^2}\right)$$

and

$$\Delta\sigma^2 = \Delta S(f_2 - f_1),$$

where R_{in}' is membrane resistance during the action of ACh. ΔS and $\Delta\sigma^2$ values would be equal to

$$\Delta S = 2 \times 10^{-26}\ \text{A}^2/\text{Hz}$$

and

$$\Delta\sigma^2 = 9 \times 10^{-24}\ \text{A}^2.$$

The minimal values of $S(f)$ at 430 Hz obtained in our experiments were equal to 2×10^{-24} A²/Hz, which exceeded ΔS by about two orders of magnitude. The corresponding values of the variances differ by about three orders of magnitude. Thus, in practice, the subtraction procedure should provide complete removal of extraneous noise contribution into the ACh noise spectrum. Another extraneous noise component, originating in the input stage of the amplifier, had the r.m.s. value of 5 μV in the frequency range 1–500 Hz, which was equivalent to a 3 MΩ resistance added to R_e and thus was negligible compared with R_e.

RESULTS

Characteristics of the e.p.s.c.

Voltage dependence of e.p.s.c. Supramaximal stimuli applied to the cervical sympathetic nerve usually evoke a multicomponent e.p.s.c. which is due to the innervation of each cell by several preganglionic fibres differing in their thresholds and conduction velocities. Only one-component e.p.s.c.s of simple shape, usually evoked by just-

threshold stimuli, were used for further analysis in this work. Their amplitudes at −80 mV ranged from 4 to 80 nA. An example of such an e.p.s.c. is shown in Fig. 1*A*. The relation between the amplitude of the e.p.s.c. and the membrane potential level was linear at the negative levels and non-linear at the positive levels of membrane potential (Fig. 1*B*). The mean value of the reversal potential was −9·6 ± 1·7 mV (S.D., $n = 7$).

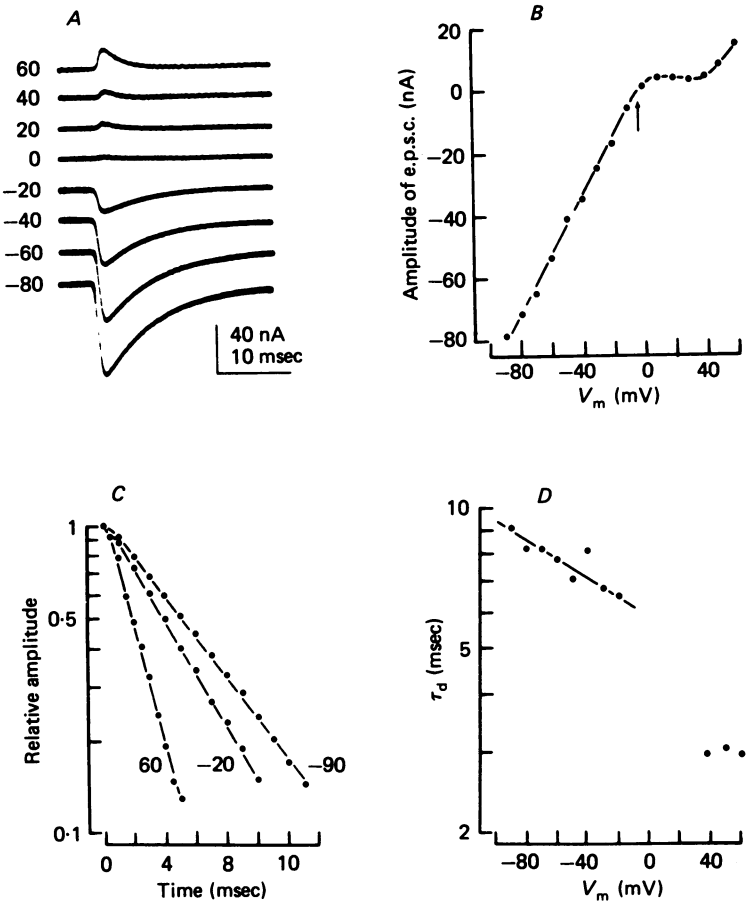

Fig. 1. Characteristics of e.p.s.c. *A*, e.p.s.c.s recorded in the same cell at different levels of membrane potential (indicated in mV near each record). *B*, peak amplitude of e.p.s.c. as a function of membrane potential (V_m). The reversal potential (arrow) is −3 mV. *C*, semilogarithmic plots of decay of three e.p.s.c.s recorded at different levels of membrane poential (indicated in mV near each plot). *D*, semilogarithmic plot of e.p.s.c. decay time constant (τ_d) as a function of membrane potential. The least-squares line fitted to the data for this cell is $\tau_d = 5{\cdot}8 \exp(-0{\cdot}0072\ V_m)$ msec. The data for the plots shown in *B*, *C* and *D* were obtained from the records some of which are shown in *A*.

The decay of the e.p.s.c. was a single-exponential as indicated by a straight-line relationship in the semilogarithmic plot of the e.p.s.c. amplitude against time (Fig. 1*C*). The mean value of the e.p.s.c. decay time constant τ_d measured in ten cells was 4·6 ± 0·4 msec. The value of τ_d increased as the membrane was hyperpolarized, an e-fold increase corresponding to about 140 mV hyperpolarization (Fig. 1*D*).

The characteristics of the e.p.s.c. described above were very close to those found in earlier experiments performed on non-atropinized neurones (Selyanko *et al.* 1979). This indicates that atropine in the concentration used (1 μM) did not affect the activity of nicotinic ACh receptor channels.

Effect of temperature on e.p.s.c. In rat parasympathetic ganglion neurones Rang (1981) has found that at room temperature (20 °C) e.p.s.c.s decay with a bi-exponential

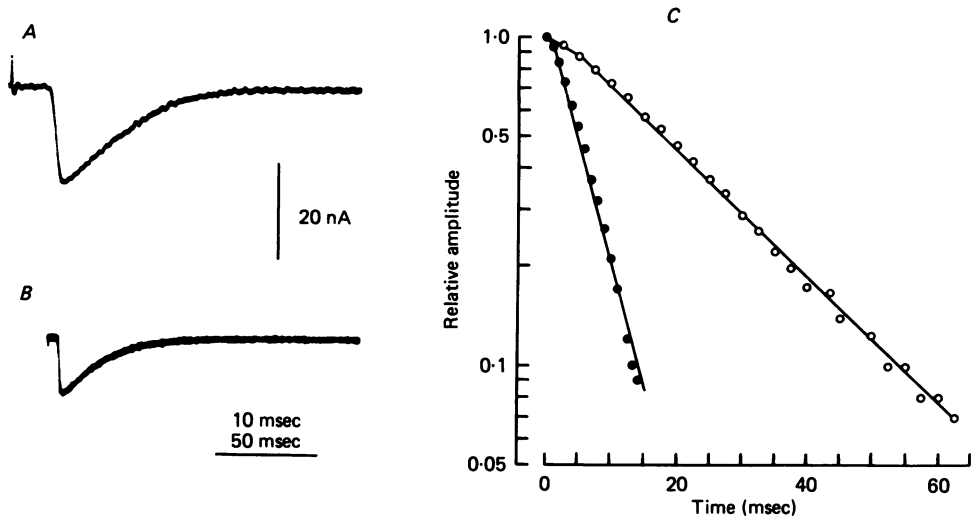

Fig. 2. Effect of temperature on e.p.s.c. The e.p.s.c.s recorded in the same neurone at 36 °C (*A*) and at 23 °C (*B*). Time calibration is 10 msec for *A* and 50 msec for *B*; current calibrations for *A* and *B* are the same. *C*, semilogarithmic plot of time courses of the e.p.s.c. decays shown in *A* (●) and in *B* (○).

time course. This contrasts with the observations reported above. One possible explanation for this discrepancy could be a masking of a fast kinetic component in the broad peak of the e.p.s.c. in our experiments at 36 °C. In order to test this possibility, the effect of low temperature on the e.p.s.c. decay was studied in five neurones. It was found that in all neurones the decay of e.p.s.c. slowed down but remained a single exponential when the temperature was reduced from 36 to 21 °C. Fig. 2 shows examples of the e.p.s.c.s recorded in the same neurone at 36 °C (*A*) and at 23 °C (*B*) and semilogarithmic plots of their decays against time (*C*). It is clearly seen that although the decay of e.p.s.c. is slowed down by a factor of 3·4 times, its time course remains a single-exponential. This indicates that the e.p.s.c. in mammalian sympathetic ganglion really differs from that in parasympathetic ganglion in its decay time course.

The temperature dependence of τ_d could be described by a linear Arrhenius plot (Fig. 3). Thus, a one-step reaction determines the duration of the e.p.s.c. decay. The high mean value of Q_{10} for τ_d ($3{\cdot}7 \pm 0{\cdot}3$, $n = 5$) suggests that diffusion of transmitter from the synaptic cleft is not a limiting factor for the rate of e.p.s.c.s decay. Similar values of Q_{10} for τ_d were found at the neuromuscular junction (Kordaš, 1972; Magleby & Stevens, 1972*b*; Gage & McBurney, 1975) and in amphibian sympathetic ganglion neurones (MacDermott *et al.* 1980). However, Kuba & Nishi (1979) obtained a higher

temperature dependence of τ_d in amphibian sympathetic ganglion neurones ($Q_{10} = 6$). Additional effects of low temperature on the e.p.s.c. were an increased rise time and a decreased amplitude (see Fig. 2). The Q_{10} values for the rise time and for the amplitude of e.p.s.c. were much lower than those for τ_d (2·3±0·6 and 1·4±0·2 respectively).

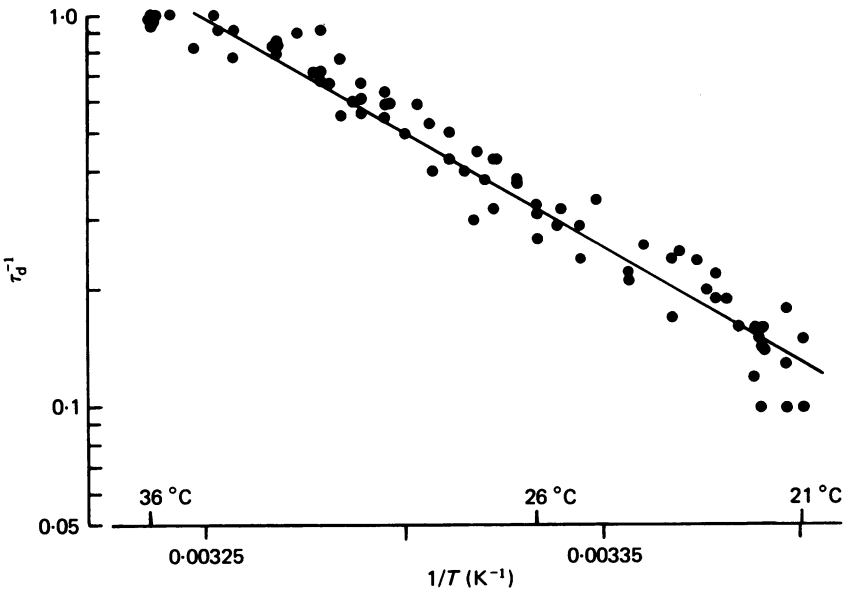

Fig. 3. Arrhenius plot of the e.p.s.c. decay rate constant (τ_d^{-1}). Data were obtained from five neurones. In each case the data were normalized about the values obtained at 36 °C.

The characteristics of the m.e.p.s.c. The decay of the e.p.s.c. might be somewhat prolonged by a time dispersion in transmitter release from the different preganglionic nerve terminals that converge upon the same neurone as well as from the terminals of a single axon. In order to evaluate the effect of this factor on the time course of the e.p.s.c., we analysed the decays of spontaneously arising m.e.p.s.c.s, assuming that synaptic inputs from different preganglionic fibres have equal probabilities to evoke m.e.p.s.c.s. At the normal K^+ concentration m.e.p.s.c.s appeared with a frequency of one m.e.p.s.c. per several seconds and their mean amplitude, measured in thirteen cells, was 0·39±0·05 nA. The quantal content of the e.p.s.c., calculated from the ratio of the evoked e.p.s.c. peak amplitude to the mean peak amplitude of the m.e.p.s.c. recorded from the same cell, ranged from 4 to 243. As illustrated by Fig. 4, both the e.p.s.c. and m.e.p.s.c. showed single-exponential decays, with very similar time-constants, τ_d and $\tau_{m,d}$. Mean values for τ_d and $\tau_{m,d}$ as measured in the same cells were 4·8±0·4 ms and 4·1±0·3 ms respectively (pooled results obtained from nine cells); the difference was statistically non-significant. Fig. 5 shows a histogram of the values for 513 m.e.p.s.c.s recorded from twelve cells. The distribution of τ_d values appears unimodal, suggesting that the e.p.s.c.s produced by different synapses do not essentially differ in their kinetics, and that the decay of e.p.s.c. is

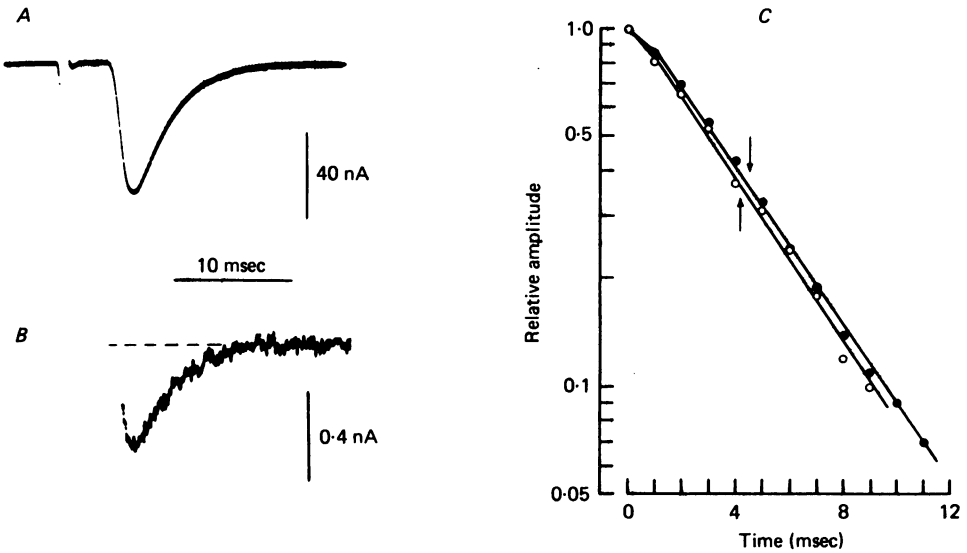

Fig. 4. Comparison of time courses of the e.p.s.c. and miniature e.p.s.c. decays. E.p.s.c. (*A*) and m.e.p.s.c. (*B*) recorded from the same cell. *C*, semilogarithmic plot of decays of e.p.s.c. (●) and m.e.p.s.c. (○) shown in *A* and *B*. The decay time constants (arrows) are 4·4 msec and 4·0 msec for e.p.s.c. and m.e.p.s.c. respectively.

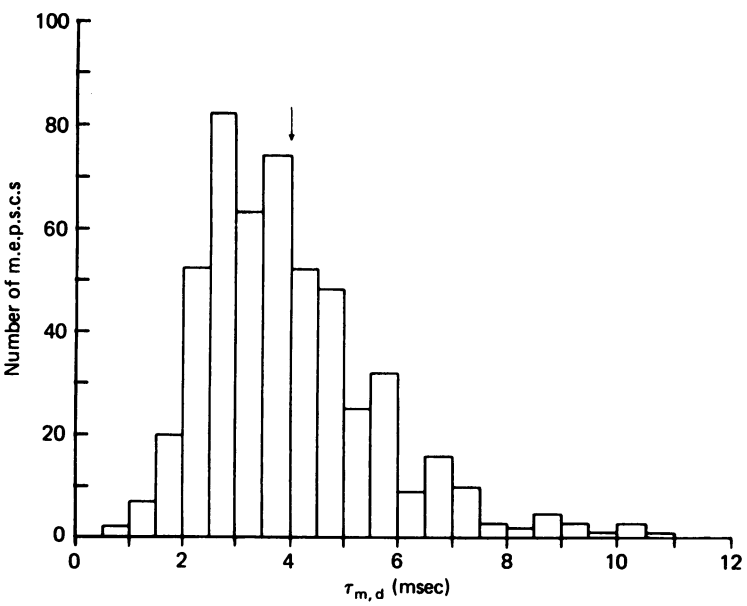

Fig. 5. Distribution of decay time constants ($\tau_{m,d}$) of 513 miniature e.p.s.c.s recorded from twelve neurones. The mean value of $\tau_{m,d}$ (arrow) is 4·0 msec.

not influenced in an appreciable way by the temporal dispersion of preganglionic nerve impulses or transmitter quanta release.

ACh noise analysis

Single channel lifetime. The application of ACh produced an inward current accompanied by the appearance of ACh noise (Fig. 6*A*, *B*). The net power spectrum

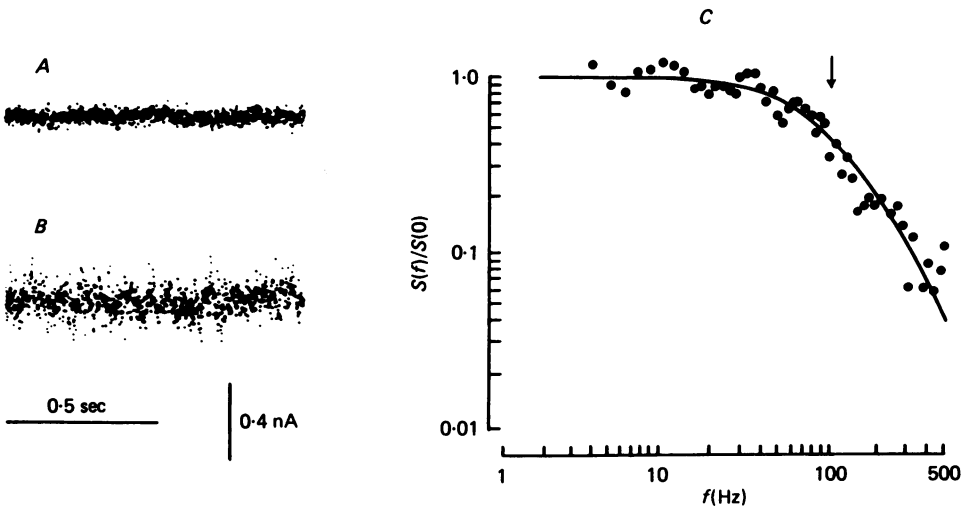

Fig. 6. Power spectrum of ACh noise fitted by Lorentzian curve. Digitalized records of current fluctuations before (*A*) and during (*B*) application of ACh. *C*, the ACh noise spectrum was obtained by subtracting the averaged spectrum of four records similar to that shown in *A* from the averaged spectrum of four records similar to that shown in *B*. The line is drawn from a least-squares fit of the points to a single Lorentzian curve. Arrow indicates the cut-off frequency (106 Hz) giving an average channel lifetime $\tau_{N_1} = 1{\cdot}5$ msec. The ACh-induced steady current was 1·4 nA.

of ACh noise shown in Fig. 6*C* was satisfactorily described by a single Lorentzian curve according to the equation (Anderson & Stevens, 1973):

$$S(f) = S(0)/(1 + (f/f_1)^2),$$

where $S(f)$ is spectral density at frequency f and f_1 is a cut-off frequency that corresponds to a $S(f)$ value half the asymptotic value $S(0)$. The mean channel lifetime τ_{N_1}, given by the equation $\tau_{N_1} = 1/2\,\pi f_1$, was, for the cell illustrated by Fig. 6, 1·5 msec. In one more neurone τ_{N_1} appeared to be close to the above value and was equal to 1·1 msec.

In the remaining fifteen neurones a much better fit to the experimental data was yielded by the sum of two Lorentzian curves, according to the equation (Dreyer, Walther & Peper, 1976; Gardner & Stevens, 1980):

$$S(f) = \{S_1(0)/(1 + (f/f_1)^2)\} + \{S_2(0)/(1 + (f/f_2)^2)\}$$

where f_1 and f_2 are the cut-off frequencies corresponding to half the asymptotic spectral densities $S_1(0)$ and $S_2(0)$. In these neurones fitting the ACh noise spectra by

a sum of two Lorentzian curves showed a statistically significant improvement over a fit using a single Lorentzian curve: the variance of the spectrum relatively to the fitted curve was $6{\cdot}7 \pm 1{\cdot}1$ times less in the former case than in the latter. The simplest explanation for this observation is a contribution of two distinct types of channels with mean lifetimes τ_{N_1} (short-living channels) and τ_{N_2} (long-living channels) equal

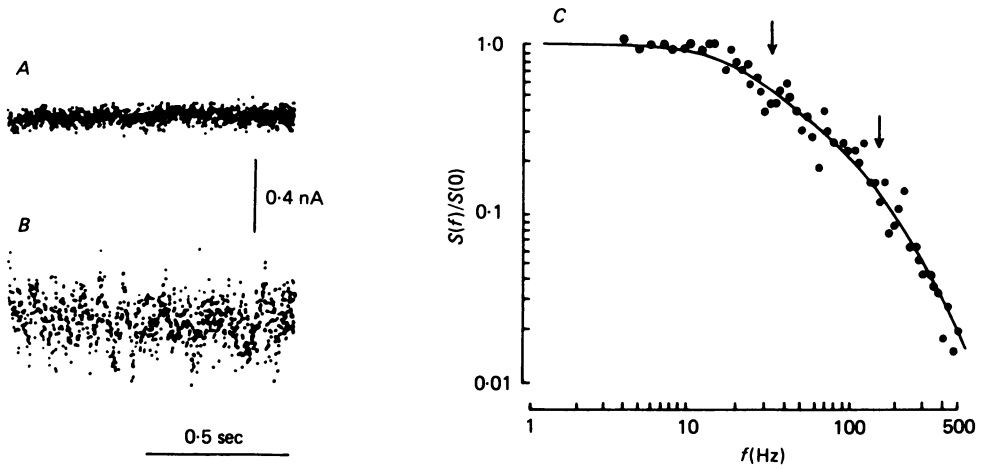

Fig. 7. Power spectrum of ACh noise fitted by the sum of two Lorentzian curves. Digitalized records of current fluctuations before (*A*) and during (*B*) application of ACh. C, ACh noise spectrum obtained by subtracting the averaged spectrum of four records similar to that shown in *A* from averaged spectrum of four records similar to that shown in *B*. The line was drawn from least-squares fit of the points to the sum of two Lorentzian curves. Arrows indicate the cut-off frequencies 145 Hz and 33 Hz giving average channel lifetimes $\tau_{N_1} = 1{\cdot}1$ msec and $\tau_{N_2} = 4{\cdot}9$ msec respectively. $S_1(0)/S_2(0)$ ratio is 0·3. The ACh-induced steady current was 3·8 nA.

to $1/2\pi f_1$ and $1/2\pi f_2$ respectively. For the double Lorentzian spectrum illustrated by Fig. 7 τ_{N_1} was 1·1msec, τ_{N_2} was 4·9 msec and the ratio $S_1(0)/S_2(0)$ was 0·3. The mean values obtained from fifteen neurones were $\tau_{N_1} = 1{\cdot}1 \pm 0{\cdot}1$ msec, and $\tau_{N_2} = 5{\cdot}0 \pm 0{\cdot}5$ msec; the ratio $S_1(0)/S_2(0)$ ranged from 0·1 to 1·0. The mean value of τ_{N_1} in the double Lorentzian spectra corresponded to the mean value of τ_{N_1} in the single-Lorentzian spectra. Similar two-Lorentzian spectra were observed in five neurones in the absence of atropine ($\tau_{N_1} = 1{\cdot}0 \pm 0{\cdot}2$ msec; $\tau_{N_2} = 5{\cdot}4 \pm 1{\cdot}1$ ms) indicating that they were not due to the effect of atropine.

To know what type of the ionic channels is involved in generating the e.p.s.c., the values of τ_{N_1} and τ_{N_2} were compared with the τ_d values measured in the same neurones. The pooled results obtained from eleven neurones were as following: $\tau_d = 4{\cdot}5 \pm 0{\cdot}3$ ms, $\tau_{N_1} = 1{\cdot}2 \pm 0{\cdot}2$ ms and $\tau_{N_2} = 5{\cdot}2 \pm 0{\cdot}6$ ms. The difference between τ_d and τ_{N_2} values was statistically non-significant. Thus the decay of the e.p.s.c. was determined by the kinetics of the longer lifetime channels.

The effect of increasing doses of ACh on channel lifetimes was studied in five cells with two-component ACh noise spectra and in two cells with single-component ACh noise spectra. No regular changes either in the absolute values of τ_{N_1} and τ_{N_2} or in

the $S_1(0)/S_2(0)$ ratio were observed. In one cell with a single-component spectrum the τ_{N_2} component appeared as the dose of ACh was increased. Fig. 8*B* shows the values of τ_{N_1} and τ_{N_2} calculated at various doses of ACh. Both values remained constant as the amplitude of ACh-induced current increased from 0·6 nA to 22 nA. It can be concluded that τ_{N_1} and τ_{N_2} values are dose-insensitive.

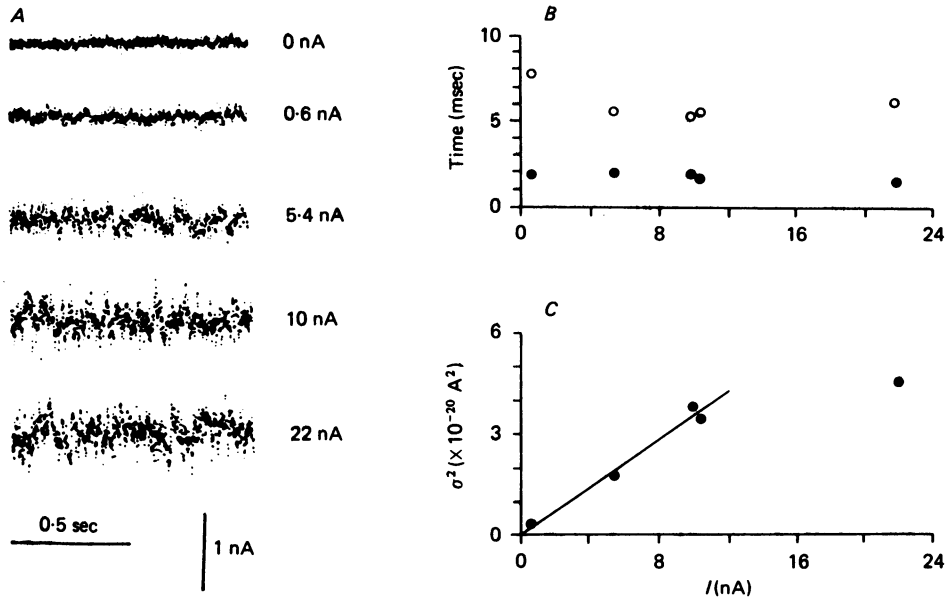

Fig. 8. Effects of increasing doses of ACh on ACh-induced current fluctuations. *A*, digitalized records of current fluctuations induced by various doses of ACh (the ACh-induced steady currents are indicated near each record). All records were obtained from the same cell. Each record is one of four similar records, from which the averaged ACh noise spectra and variances were obtained. Mean channel lifetimes τ_{N_1} (●) and τ_{N_2} (○) (*B*) and variance σ^2 of current fluctuations (*C*) are plotted as functions of mean ACh-induced current (*I*). The $S_1(0)/S_2(0)$ ratio was 0·3 at all values of *I*. σ^2 was linearly related to *I* at values of *I* not exceeding 10 nA. The slope of the regression line gives the single channel current of 3·7 pA.

Single channel conductance. From the mean ACh-induced steady membrane current, *I*, and the ACh noise variance, σ^2, the elementary current pulse flowing through a single channel, *i*, was calculated using the equation (Anderson & Stevens, 1973) $i = \sigma^2/I$.

Fig. 8*C* shows that the σ^2 value increases linearly as *I* increases up to 10 nA; the *i* value estimated from the slope of this relationship is 3·7 pA. The mean *i* value was $2{\cdot}7 \pm 0{\cdot}2$ pA ($n = 17$). The σ^2 to *I* ratio remained constant in the same range of membrane currents (up to 10 nA) in six other neurones tested. This indicates that the concentration of ACh applied did not exceed the low concentration limit (Katz & Miledi, 1972; Anderson & Stevens, 1973). The σ^2 values of ACh noise usually were eight to twenty times higher than those of the background noise recorded in the absence of ACh.

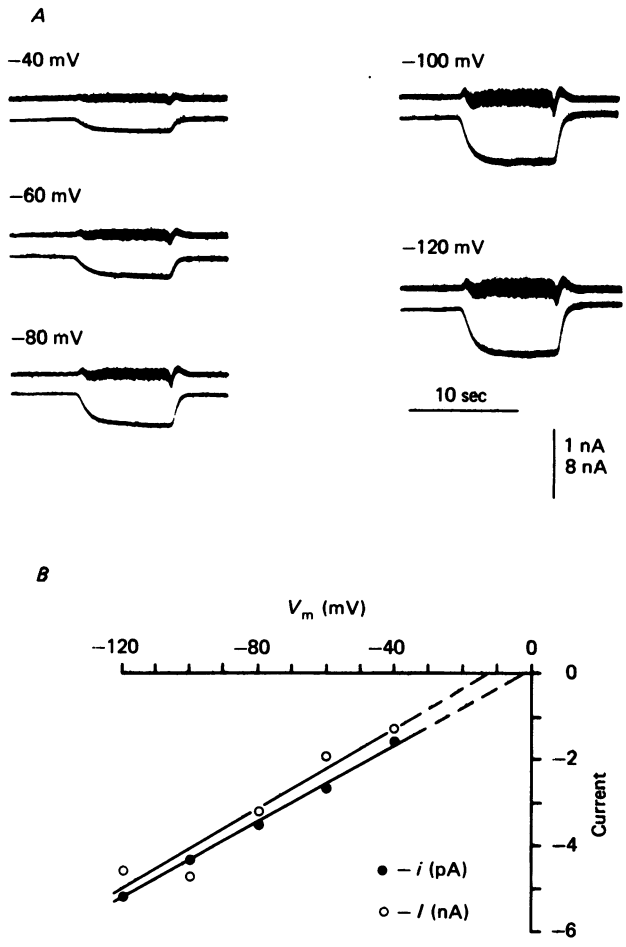

Fig. 9. Voltage dependence of ACh-induced steady-state and single channel currents. *A*, membrane currents induced by ionophoretic application of ACh as recorded at different levels of membrane potential (indicated in mV near each record) in the same cell. The lower trace in each record is the ACh-induced current recorded in frequency range 0–430 Hz at low gain. The upper trace is the same current recorded in frequency range of 1–430 Hz at high gain. *B*, ACh-induced steady current (*I*) and single channel current (*i*) plotted against the membrane potential. Extrapolated values of the reversal potential are −13 mV and −2 mV for *I* and *i* respectively. The graph data was obtained from analysis of the records shown in *A*.

The single channel conductance, γ, was calculated from the equation $\gamma = i/(V_m - V_r)$, where V_m is holding membrane potential, and V_r is the reversal potential. In some of the neurones studied the amplitude of the ACh-induced steady current I was almost linearly related to the membrane potential, and V_r for both I and i values could be estimated using an extrapolation method. In the example shown in Fig. 9, $I(V)$ and $i(V)$ relationships slightly differ in their slopes yielding extrapolated V_r values of −13 and −2 mV respectively. A difference in the same direction in the V_r values was observed in all neurones studied. However, this

difference was higher in the cells with obviously non-linear I–V relationships. The mean extrapolated V_r value for i was $+1{\cdot}1 \pm 5{\cdot}2$ mV ($n = 7$).

It seems likely that a difference between the V_r values for I and for i is due to the error introduced by the extrapolation method. The slope of I–V relationship is apparently affected by two factors: (i) voltage dependence of channel lifetime (see Dionne & Stevens, 1975; Mallart, Dreyer & Peper, 1976) and (ii) development of a K^+ current induced by entry of Ca^{2+} into the cell during the ACh response (see Meech, 1974; Ascher, Marty & Neild, 1978*a*). The voltage dependence of channel lifetime should be given by the voltage dependence of τ_d. The development of a K^+ current during ACh response is suggested by the facts that Ca^{2+} is involved in the ACh response in sympathetic neurones (Pappano & Volle, 1966; Koketsu, Nishi & Soeda, 1968) and that the entry of Ca^{2+} into the cell augments K^+ conductance in these neurones (McAfee & Yarowsky, 1979). The first factor should lead to an increase of I with membrane hyperpolarization and the second one should result in a decrease of inward I with membrane depolarization; thus both factors should increase the slope of I–V relationship. The real values of V_r for I are apparently less negative and close to V_r values for e.p.s.c.. Ascher *et al.* (1978*a*) observed in *Aplysia* neurones that the K^+ current was not accompanied by noise and so i values at less negative membrane potentials were overestimated due to underestimation of ACh-induced steady current. If this is so in sympathetic neurones, the real V_r value for i should be more negative than that found by extrapolation and thus it apparently approaches the above value of V_r for e.p.s.c.

Assuming V_r for i is -10 mV and the short- and long-living channels have similar single-channel conductances, the γ value obtained was equal to 36 ± 3 pS. The values of γ estimated in two neurones with single-Lorentzian spectra (35 pS and 44 pS) were not very different from those obtained for total population of neurones indicating that the second assumption was true. This means that the contributions of the two components in the total variance are equal to their contributions to total steady current. The contribution of the τ_{N_1}-component to the total variance

$$\sigma_1^2 = \frac{S_1(0)}{4\tau_{N_1}}$$

varied in different neurones from 32 to 91 % with the mean value of $65{\cdot}7 \pm 6{\cdot}1$ %. Thus, in two-component spectra the contribution to the ACh response of short- was higher than that of long-living channels.

Effect of temperature on single channel lifetime and conductance. The effect of low temperature on τ_{N_1}, τ_{N_2} and γ was studied in four neurones. In these experiments the ACh-induced current fluctuations were recorded within extended frequency range (0·25 Hz to 430 Hz), and the net ACh noise spectrum was obtained from an increased number of records (eight records) and was fitted by Lorentizian curves within the extended frequency range (1 to 350 Hz).

Fig. 10 shows power spectra of ACh noise recorded in the same neurones at 36 and 24 °C. It is seen that at room temperature the power spectrum remains double Lorentzian and both τ_{N_1} and τ_{N_2} are slowed down. The mean values of τ_{N_1} and τ_{N_2} were $1{\cdot}1 \pm 0{\cdot}1$ msec ($n = 4$) and $7{\cdot}1 \pm 0{\cdot}9$ msec ($n = 4$) at 36 °C and they were slowed by lowering the temperature in the range between 36 and 20 °C according to the

Arrhenius equation with the Q_{10} equal to $2{\cdot}8 \pm 0{\cdot}4$ and $2{\cdot}9 \pm 0{\cdot}4$ for τ_{N_1} and τ_{N_2} respectively. Thus, the temperature dependences of τ_{N_1} and τ_{N_2} are similar, and are close to that of τ_d (see above). The differences between τ_{N_1}, τ_{N_2} and τ_d are not statistically significant. The values of γ were almost unchanged in the range between 36 and 21 °C, but dropped suddenly as the temperature was lowered below 21 °C, as observed in other nicotinic ACh receptors (Fischbach & Lass, 1978).

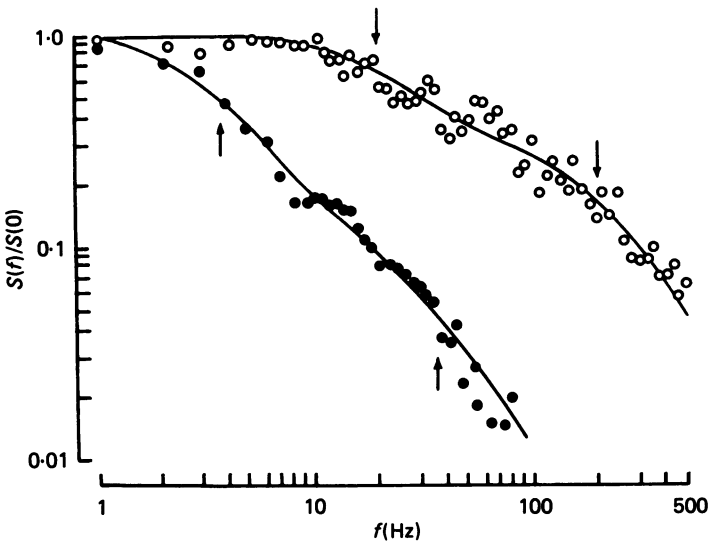

Fig. 10. Effect of temperature on power spectrum of ACh noise. Power spectra of ACh noise were recorded in the same neurone at 36 °C (○) and at 24 °C (●). Each line was drawn from least-squares fit of the points to the sum of two Lorentzian curves. Arrows indicate the cut-off frequencies 198 Hz and 19·5 Hz giving average channel lifetimes $\tau_{N_1} = 0{\cdot}8$ msec and $\tau_{N_2} = 8{\cdot}2$ msec (at 36 °C) and 35·1 Hz and 3·7 Hz giving average channel lifetimes $\tau_{N_1} = 4{\cdot}5$ msec and $\tau_{N_2} = 43{\cdot}5$ msec (at 24 °C).

The effect of α-bungarotoxin

The fact that the slow kinetic component of ACh noise spectra is the only one controlling the e.p.s.c. decay, suggests that the transmitter liberated by the presynaptic terminal does not activate short-living channels, and that these channels are probably extrasynaptic. Recently Dun & Karczmar (1980) reported that α-bungarotoxin selectively blocked the ACh potential without affecting the e.p.s.p. in sympathetic neurones, thus suggesting that only extrasynaptic ACh receptors were sensitive to α-bungarotoxin. One thus could expect that the ACh-induced current (but not the e.p.s.c.) and the contribution of fast kinetic component to ACh noise spectra both should be selectively depressed by α-bungarotoxin. In order to test this assumption, we studied the effect of α-bungarotoxin (1 μM) on the e.p.s.c., the ACh-induced current and the ACh noise spectra. It was found that α-bungarotoxin depressed both the ACh response (by 79%, as an average in six neurones, from six different preparations) and the e.p.s.c. (by 44%, as an average in four neurones, from four different preparations). Therefore, α-bungarotoxin is not a selective antagonist for

extrasynaptic ACh receptors. In addition, α-bungarotoxin caused no regular changes in the contribution of fast kinetic component to ACh noise spectra.

DISCUSSION

The results presented in this work show that there are two distinct kinetics – fast and slow – in the nicotinic ACh receptor channels of mammalian sympathetic ganglion neurones. Similar observations were made in some other cells possessing nicotinic ACh receptors: in skeletal muscle fibres (Dreyer *et al.* 1976; Neher & Sakmann, 1976; Dionne & Parsons, 1981), in *Aplysia* neurones (Gardner & Stevens, 1980) and in rat parasympathetic ganglion neurones (Rang, 1981). The origin of two channel kinetics in sympathetic ganglion neurones could be explained in two different ways: (i) there are channels with multiple states, and (ii) there are two distinct populations of channels, with short and long lifetimes respectively.

Some examples of multiple channel kinetics were shown by Neher & Steinbach (1978), Nelson & Sachs (1979), Sakmann, Patlak & Neher (1980), and Dionne (1981). The models of multiple channel kinetics predict that the contribution of the fast kinetic component to ACh noise spectra should be dependent on the dose of ACh and that the slow kinetic component should be present in all ACh noise spectra. In as much as this is not consistent with our observations, the explanation (ii) about two populations of channels with short and long lifetimes of their opened states is more likely.

In the present study the slow kinetic component in ACh noise spectrum was equal in its duration to the e.p.s.c. decay time-constant. This indicates that the open channel lifetime is the main factor determining the duration of e.p.s.c. decay, as found earlier in other nicotinic synapses (Katz & Miledi, 1972; Anderson & Stevens, 1973; Gardner & Stevens, 1980; Dionne & Parsons, 1981; Rang, 1981). This conclusion is supported by some previous indirect observations: the voltage dependence of the e.p.s.c. decay (Selyanko et al. 1979) and the voltage-dependent shortening of the e.p.s.c. decay in the presence of hexamethonium and tubocurarine (Selyanko, Derkach & Skok, 1981) which are commonly considered as channel-blocking agents (Ascher, Marty & Neild, 1978*b*; Ascher, Large & Rang, 1979; Colquhoun, Dreyer & Sheridan, 1979). At room temperature the lifetime of ionic channels in mammalian sympathetic ganglion neurones is a few times longer than in amphibian sympathetic ganglion neurones (cf. Kuba & Nishi, 1979; MacDermott *et al.* 1980), about thirty times longer than at the neuromuscular junction (see Colquhoun, 1979), and close to the lifetime of channels in molluscan neurones (Ascher *et al.* 1978*a*) and rat parasympathetic ganglion neurones (Rang, 1981).

In contrast to rat parasympathetic ganglion neurones where two kinetic components of ACh-induced spectrum were found in e.p.s.c. decay (Rang, 1981), only the slow kinetic component was found in e.p.s.c. decay in the pesent study. There are two possible explanations for this discrepancy: (i) the fast kinetic component in ACh noise spectrum corresponds to a fast decaying component of the e.p.s.c. which was not evoked by threshold stimuli used in this work; and (ii) the receptors which operate the fast channels are extrasynaptic. The first explanation is not supported by the results of the analysis of the m.e.p.s.c. decay, which was similar to that in e.p.s.c. It thus seems likely that fast channels are operated by extrasynaptic ACh receptors.

The mean amplitude of m.e.p.s.c. in sympathetic ganglion neurones measured in the present study was about one order of magnitude lower than in neuromuscular junction (Gage & McBurney, 1975; Colquhoun, Large & Rang, 1977). This correlates with a difference in the conductance change produced by a single ACh quantum obtained by the indirect method (Hunt & Nelson, 1965; Nishi, Soeda & Koketsu, 1967). Assuming that ganglionic and neuromuscular synapses do not differ in quantal ACh content (cf. Nishi *et al.* 1967) and in single channel conductance (present data; for comparison see Colquhoun, 1979), the lower effectiveness of the ACh quantum in ganglionic synapses can be explained by a smaller number of ionic channels opened at the peak of m.e.p.s.c. Relations between m.e.p.s.c. and single channel current similar to those observed in this work were found in rat parasympathetic ganglion neurones (Rang, 1981). Using another criterion for the effectiveness of transmitter action, the amount of charge transferred across the open channels (Gardner, 1980), a much smaller difference in the effectiveness of an ACh quantum between the ganglionic and neuromuscular synapses can be predicted because of the longer channel lifetime and m.e.p.s.c. decay in sympathetic ganglion neurones.

We are grateful to Professors D. A. Brown and H. P. Rang for helpful advice and discussions.

REFERENCES

ANDERSON, C. R. & STEVENS, C. F. (1973). Voltage clamp analysis of acetylcholine produced end-plate current fluctuations at frog neuromuscular junction. *J. Physiol.* **235**, 655–691.

ASCHER, P., MARTY, A. & NEILD, T. O. (1978*a*). Lifetime and elementary conductance of channels mediating the excitatory effects of acetylcholine in *Aplysia* neurones. *J. Physiol.* **278**, 177–206.

ASCHER, P., MARTY, A. & NEILD, T. O. (1978*b*). The mode of action of antagonists on the excitatory response to acetylcholine in *Aplysia* neurones. *J. Physiol.* **278**, 207–235.

ASCHER, P., LARGE, W. A. & RANG, H. P. (1979). Studies on the mechanism of action of acetylcholine antagonists on rat parasympathetic ganglion cells. *J. Physiol.* **295**, 139–170.

COLQUHOUN, D. (1979). The link between drug binding and response: theories and observations. In *The Receptors: a Comprehensive Treatise*, vol. 1, ed. O'BRIEN, R. D., pp. 93–142. New York: Plenum.

COLQUHOUN, D., DREYER, F. & SHERIDAN, R. E. (1979). The action of tubocurarine at the frog neuromuscular junction. *J. Physiol.* **293**, 247–284.

COLQUHOUN, D., LARGE, W. A. & RANG, H. P. (1977). An analysis of the action of false transmitter at the neuromuscular junction. *J. Physiol.* **266**, 361–395.

DERKACH, V. A., SELYANKO, A. A. & SKOK, V. I. (1981). Analysis of acetylcholine noise in mammalian sympathetic ganglion neurones. *Dokl. Akad. Nauk SSSR* **259**, 981–984 (in Russian).

DIONNE, V. E. (1981). The kinetics of slow muscle acetylcholine-operated channels in the garter snake. *J. Physiol.* **310**, 159–190.

DIONNE, V. E. & STEVENS, C. F. (1975). Voltage dependence of agonist effectiveness at the frog neuromuscular junction: resolution of a paradox. *J. Physiol.* **251**, 245–270.

DIONNE, V. E. & PARSONS, R. L. (1981). Characteristics of the acetylcholine channel in twitch and slow fibre neuromuscular junctions of the garter snake. *J. Physiol.* **310**, 145–158.

DREYER, F., WALTHER, CHR. & PEPER, K. (1976). Junctional and extrajunctional acetylcholine receptors in normal and denervated frog muscle fibres. Noise analysis experiments with different agonists. *Pflügers Arch.* **366**, 1–9.

DUN, N. J. & KARCZMAR, A. G. (1980). Blockade of ACh potentials by α-bungarotoxin in rat superior cervical ganglion cells. *Brain Res.* **196**, 536–540.

FISCHBACH, G. D. & LASS, Y. (1978). A transition temperature for acetylcholine channel conductance in chick myoballs. *J. Physiol.* **280**, 527–536.

GAGE, P. W. & MCBURNEY, R. N. (1975). Effects of membrane potential, temperature and neostigmine on the conductance change caused by a quantum of acetylcholine at the toad neuromuscular junction. *J. Physiol.* **244**, 385–407.

GARDNER, D. (1980). Time integral of synaptic conductance. *J. Physiol.* **304**, 181–191.

GARDNER, D. & STEVENS, C. F. (1980). Rate-limiting step of inhibitory post-synaptic current decay in *Aplysia* buccal ganglia. *J. Physiol.* **304**, 145–164.

HUNT, C. C. & NELSON, P. G. (1965). Structural and functional changes in the frog sympathetic ganglion following cutting of the presynaptic nerve fibres. *J. Physiol.* **177**, 1–20.

KATZ, B. & MILEDI, R. (1972). The statistical nature of the acetylcholine potential and its molecular components. *J. Physiol.* **224**, 665–699.

KOKETSU, K., NISHI, S. & SOEDA, H. (1968). Calcium and acetylcholine-potential of bullfrog sympathetic ganglion cell membrane. *Life Sci. Oxford* **7**, 955–963.

KORDAŠ, M. (1972). An attempt at an analysis of the factors determining the time course of the end plate current. I. The effects of prostigmine and the ratio of Mg^{2+} to Ca^{2+}. *J. Physiol.* **224**, 317–332.

KUBA, K. & NISHI, S. (1979). Characteristics of the fast excitatory postsynaptic current in bullfrog sympathetic ganglion cells. Effects of membrane potential, temperature, and Ca ion. *Pflügers Arch.* **378**, 205–212.

MACDERMOTT, A. B., CONNOR, E. A., DIONNE, V. E. & PARSONS, R. L. (1980). Voltage clamp study of fast excitatory synaptic currents in bullfrog sympathetic ganglion cells. *J. gen. Physiol.* **75**, 39–60.

MAGLEBY, K. L. & STEVENS, C. F. (1972*a*). The effect of voltage on the time course of end-plate currents. *J. Physiol.* **223**, 151–171.

MAGLEBY, K. L. & STEVENS, C. F. (1972*b*). A quantitative description of end-plate currents. *J. Physiol.* **223**, 173–197.

MALLART, A., DREYER, F. & PEPER, K. (1976). Current-voltage relation and reversal potential at junctional and extrajunctional ACh receptors at the frog neuromuscular junction. *Pflügers Arch.* **362**, 43–47.

MCAFEE, D. A. & YAROWSKY, P. J. (1979). Calcium-dependent potentials in the mammalian sympathetic neurone. *J. Physiol.* **290**, 507–523.

MEECH, R. W. (1974). The sensitivity of *Helix aspersa* neurones to injected calcium ions. *J. Physiol.* **237**, 259–278.

NEHER, E. & SAKMANN, B. (1976). Noise analysis of drug induced voltage clamp currents in denervated frog muscle fibres. *J. Physiol.* **258**, 705–729.

NEHER, E. & STEINBACH, J. H. (1978). Local anaesthetics transiently block currents through single acetylcholine-receptor channels. *J. Physiol.* **277**, 153–176.

NELSON, D. J. & SACHS, F. (1979). Single ionic channels observed in tissue-cultured muscle. *Nature, Lond.* **282**, 861–863.

NISHI, S., SOEDA, H. & KOKETSU, K. (1967). Release of acetylcholine from sympathetic preganglionic nerve terminals. *J. Neurophysiol.* **30**, 114–134.

PAPPANO, A. J. & VOLLE, R. L. (1966). Observations on the role of calcium ions in ganglionic responses to acetylcholine. *J. Pharmac. exp. Ther.* **153**, 171–180.

RANG, H. P. (1981). The characteristics of synaptic currents and responses to acetylcholine or rat submandibular ganglion cells. *J. Physiol.* **311**, 23–55.

SAKMANN, B., PATLAK, J. & NEHER, E. (1980). Single acetylcholine-activated channels show burst-kinetics in presence of desensitizing concentrations of agonist. *Nature, Lond.* **286**, 71–73.

SELYANKO, A. A., DERKACH, V. A. & SKOK, V. I. (1979). Fast excitatory postsynaptic currents in voltage-clamped mammalian sympathetic ganglion neurones. *J. Autonomic Nervous System* **1**, 127–137.

SELYANKO, A. A., DERKACH, V. A. & SKOK, V. I. (1981). Effects of some ganglion-blocking agents on fast excitatory postsynaptic currents in mammalian sympathetic ganglion neurones. In *Adv. Physiol. Sci.*, vol. 4, *Physiology of Excitable Membranes*, ed. SALANKI, J., pp. 329–342. New York: Pergamon Press.

SKOK, V. I. (1973). *Physiology of Autonomic Ganglia*. Tokyo: Igaku Shoin Ltd.

SKOK, V. I., SELYANKO, A. A. & DERKACH, V. A. (1981). Acetylcholine noise and synaptic currents induced by activation of nicotinic receptors in mammalian sympathetic ganglion neurones. In *Physiology of Autonomic Ganglia*, ed. SKOK, V. I., p. 73. Kiev; Naukova Dumka.

TAKEUCHI, A. & TAKEUCHI, N. (1959). Active phase of frog's end-plate potential. *J. Neurophysiol.* **22**, 395–411.